A theory of the interionic structure of graphite intercalation synthetic metals: Variations with respect to interactions and state

ZhuoMin Chen, Omar A. Karim, and B. Montgomery Pettitt

Citation: The Journal of Chemical Physics **89**, 1042 (1988); doi: 10.1063/1.455255
View online: http://dx.doi.org/10.1063/1.455255
View Table of Contents: http://scitation.aip.org/content/aip/journal/jcp/89/2?ver=pdfcov
Published by the AIP Publishing

A theory of the interionic structure of graphite intercalation synthetic metals: Variations with respect to interactions and state

Zhuo-Min Chen, Omar A. Karim,[a] and B. Montgomery Pettitt
Department of Chemistry, University of Houston, Houston, Texas 77004

(Received 10 March 1988; accepted 1 April 1988)

A statistical mechanical theory is developed and applied to study the structural effects that the thermodynamic state of alkali ions have on graphite intercalation compounds. The system considered is that of second stage Rb–graphite. Two-dimensional diffraction patterns are computed and compared with experimental measurements. Sensitivity to model parameters are considered. A low order density functional expansion is found to adequately describe the interionic structure of the system modeled as a two-dimensional one component plasma in an anisotropic external field.

I. INTRODUCTION

Our knowledge of the interesting properties of the synthetic metals or the intercalation compounds of graphite has recently multiplied manyfold due to a rekindled experimental interest.[1] Using the techniques of statistical mechanics,[2–4] theories may now be developed and applied to study the effects that various alkali ions have on the structure, thermodynamics, and dynamics of graphite intercalation compounds. A theoretical understanding of the phenomena of staging and the concomitant phase transitions involve interlayer distribution functions. Thus, the details of the interionic and intermolecular distributions within the graphite layers must first be understood before the multiple layer problems may be approached at the atomic level of description.

The goal of the present study is to develop and implement new theoretical methods for exploring the equilibrium properties of graphite intercalation compounds which will be useful in understanding the relation between their structure and their associated physical properties, especially the observed catalytic activity.[5] An accurate structural theory will allow the calculation of the thermodynamics of graphite intercalation compounds, and will show how free energy differences and ion solubilities are related to the registration of the graphite layers.

A detailed understanding of these facets of lamellar graphite compounds is of fundamental importance to our understanding of the modulation and regulation of a number of organic reactions which these materials catalyze. It is widely recognized that alkali graphite compounds are active as hydrogenation catalysts for unsaturated hydrocarbons.[5] These materials are also known to catalyze polymerization in a variety of unsaturated organic compounds.[6] The most interesting structural aspect of these reactions is that the alkali metal cations are thought to be one of the major centers of the catalytic activity. Thus, the reactant organic molecules must penetrate or intercalate between the layers of graphite as well.

Synthetic metals of the graphite intercalation class are made by inserting alkali atoms between the layers of graphite. Such materials display a rich variety of physical properties which are quite distinct from the ordinary or true metals. These compounds have a remarkable thermodynamic phase diagram due to the phenomena of staging.[1,7] In general, a stage-n compound has n intervening layers of graphite between the layers of alkali metal atoms. Many physical properties vary sharply with a change in stage such as band structure, conductivity (and superconductivity), specific volume, and catalytic activity.

A great deal of recent effort has been devoted to the electronic properties of these materials.[7] Many of those studies must treat the intercalant atoms as impurities in the calculation. Some approaches have been based on assumptions of the unit cell structure, although the majority deal with isolated fragments of the structure. While such calculations provide a great deal of model information about the charge distribution in these systems, a thermodynamic understanding based on the atomic properties is lacking.

An accurate theory of the microscopic structure used with classical statistical thermodynamics would yield a precise picture of the free energy or chemical potential as a function of the geometric and interaction parameters of the system. Thus, the ultimate goal of the present study is to formulate and use density functional and integral equation theories of the structure to predict many aspects of the material's thermodynamic properties.

In this work we shall study the variation of the singlet and pair density distributions as a function of thermodynamic state (density and temperature) and interaction potential parameters. The physical–chemical object of study for this paper will be rubidium–graphite in the second stage; these compounds are experimentally well-characterized and, therefore, will prove valuable in establishing the reliability of the techniques to be used. The equilibrium distributions so calculated will be compared with various experimental measurements, most notably from x-ray diffraction measurements.[8–11]

In Sec. II the theoretical methods and models to be used will be outlined. Subsequently, the results of our study will be presented with the discussion and conclusions following. The numerical methods are presented in the Appendix.

II. THEORY

The model we use for the registered layers of graphite acting on the intercalated fluid of ions is a system composed

[a] Present address: Chemistry Dept., University of California at Berkeley, Berkeley, CA.

0021-9606/88/141042-07$02.10

of a two-dimensional fluid in the presence of an external potential. We have chosen to model the total potential energy for the system $U(\{\mathbf{r}_i\})$ as consisting of a sum of one body and two body terms. The one body potential, $U^{(1)}(\mathbf{r}_i)$, contains the two-dimensional periodically varying interaction of the graphite layers acting on the ith ion. The two body portion of the potential, $U^{(2)}(\mathbf{r}_i,\mathbf{r}_j)$, represents the effective interionic interactions in the system. The total model potential energy of the system is thus taken to be

$$U(\{\mathbf{r}_i\}) = \sum_i U^{(1)}(\mathbf{r}_i) + \sum_{i>j} U^{(2)}(\mathbf{r}_i,\mathbf{r}_j) \,. \tag{1}$$

The position of atom (ion) i is denoted $\mathbf{r}_i$ and $\{\mathbf{r}_i\}$ represents the collection of all coordinates $\mathbf{r}_i$. In this equation the summations extend over all ions in the two-dimensional system.

As this system is anisotropic we must choose a convenient coordinate system. Employing a low order Fourier expansion of $U^{(1)}(\mathbf{r}_i)$ we chose a two-dimensional Cartesian coordinate system (x,y) consistent with the one body contributions defined as

$$U^{(1)}(\mathbf{r}) = 2K\left\{2\cos\left[\left(\frac{2\pi}{a}\right)x\right]\cos\left[\left(\frac{2\pi}{a}\right)\frac{1}{\sqrt{3}}y\right] + \cos\left[\left(\frac{2\pi}{a}\right)\frac{2}{\sqrt{3}}y\right]\right\} . \tag{2}$$

Here, the lattice constant is given by $a=\sqrt{3}\,d$, where d is the distance between repulsive graphitic carbon centers. This choice of $U^{(1)}$ gives the major features of the registered graphite lattice interaction with the ions while exhibiting the requisite translational invariance along lattice vectors and the local sixfold symmetry.

The choice of $U^{(2)}$ is governed not only by the Coulombic interactions between bare ions but by the nature of the electronic interactions between the intercalant and the graphite sheets, giving rise to the intralayer screening. In the case of alkali atoms, evidence from electronic structure calculations and other sources indicates that there is an electron transfer from the alkali to the graphite.[12–15] Thus, we have taken the two body interaction to be that of a screened Coulomb or Yukawa form:

$$U^{(2)}(\mathbf{r}_1,\mathbf{r}_2) = q_1 q_2 \exp(-\varkappa|\mathbf{r}_1-\mathbf{r}_2|)\,|\mathbf{r}_1-\mathbf{r}_2|^{-1} . \tag{3}$$

As all of the ions are of the same charge q this potential is purely repulsive. For realistic choices of the screening parameter $\varkappa$ no hard-core nor Lennard-Jones r^{-12}-type of repulsion was found necessary for our qualitative level of comparison with experiment. It is true that more adjustable terms in the potential would allow greater flexibility in fitting the experimental data; however, that is not the goal of the present work. In very dense, two-dimensional systems such a strong repulsive term may certainly be necessary. The simplistic form of the potential we have chosen allows for a clear analysis of the effects on the observable properties upon changing the independent model constants K and $\varkappa$ as well as the thermodynamic variables of state.

The most vivid experimental data on the structure of graphite intercalation complexes are given by recent diffraction experiments.[8] Comparison with this data requires only the singlet and pair density distributions. This sort of information, in principle, is available from hierarchal equations.[16] Such an approach would require an approximate closure or truncation of the hierarchy. Instead, the one body distribution and the pair correlations may be approximated by simultaneously solving the anisotropic Ornstein–Zernike (OZ) equation with an approximate closure expression and an equation that relates the singlet distribution function to the pair distribution function.

For an anisotropic system we may write the OZ equation as

$$h^{(2)}(\mathbf{r}_1,\mathbf{r}_2) = c^{(2)}(\mathbf{r}_1,\mathbf{r}_2) + \int c^{(2)}(\mathbf{r}_1,\mathbf{r}_3)\rho(\mathbf{r}_3)h^{(2)}(\mathbf{r}_3,\mathbf{r}_2)d\mathbf{r}_3 , \tag{4}$$

where $c^{(2)}$ is the OZ direct correlation function and may be taken to be defined by this equation. The pair correlation function is denoted by $h^{(2)}$ and ρ is the r-dependent singlet density distribution function. A variety of approximate closure relations may be used with the OZ equation. The functional form of the pair potential chosen allows for formally long ranged interactions and even for nonzero $\varkappa$ the effective range of the potential may be quite long. Thus, based on the literature for isotropic three-dimensional fluids we chose the hypernetted chain (HNC) closure over alternatives such as the Percus–Yevick (PY) relation.[16] The anisotropic HNC closure is given by

$$c^{(2)}(\mathbf{r}_1,\mathbf{r}_2) = \exp[-\beta U^{(2)}(\mathbf{r}_1,\mathbf{r}_2) + h^{(2)}(\mathbf{r}_1,\mathbf{r}_2) - c^{(2)}(\mathbf{r}_1,\mathbf{r}_2)] - h^{(2)}(\mathbf{r}_1,\mathbf{r}_2) + c^{(2)}(\mathbf{r}_1,\mathbf{r}_2) - 1 . \tag{5}$$

$\beta = 1/k_B T$ with k_B the Boltzmann constant and T the absolute temperature. The OZ relation [Eq. (4)] and the HNC [Eq. (5)] thus give an approximate representation of the pair correlations in an anisotropic fluid given a nonconstant $\rho(\mathbf{r})$.

To proceed, a relation between the singlet and pair distributions is needed. For our calculation for a nonisotropic fluid we start with the exact Lovet–Mou–Buff equation[17]

$$\nabla_1\{\ln[\rho(\mathbf{r}_1)] + \beta U^{(1)}(\mathbf{r}_1)\} = -\int \rho(\mathbf{r}_2)\nabla_2 c^{(2)}(\mathbf{r}_1,\mathbf{r}_2)d\mathbf{r}_2 . \tag{6}$$

In principle, Eqs. (4), (5), and (6) form a closed set of relations and can be solved for the one and two particle correlation functions. Such a solution is, however, tedious and time consuming. In order to circumvent these numerical difficulties, we consider a perturbation expansion of $c^{(2)}(\mathbf{r}_1,\mathbf{r}_2)$ using an isotropic reference system. That is, the reference system is chosen to be identical to the system described by the interactions in Eq. (1) with the one body term removed. Quantities relating to the reference system will carry a subscript "0." Thus the reference system is an unmodulated liquid with a density ρ_0 identical to the bulk density of the modulated liquid. Hence, $\rho(\mathbf{r})$ must satisfy

$$\frac{1}{V}\int \rho(r)d\mathbf{r} = \rho_0 , \tag{7}$$

where V is the volume (or area) of integration which, in practice, should be large compared to the periodicity of $U^{(1)}$.

Next, we consider an expansion of the direct correlations about that of the reference system.[18,19] In terms of the isotropic reference system, the functional Taylor expansion of $c^{(2)}(\mathbf{r}_1,\mathbf{r}_2)$ yields

$$c^{(2)}(\mathbf{r}_1,\mathbf{r}_2) = c_0^{(2)}(r_{12}) + \int c_0^{(3)}(\mathbf{r}_1,\mathbf{r}_2,\mathbf{r}_3) \times [\rho(\mathbf{r}_3) - \rho_0]d\mathbf{r}_3 + \cdots . \quad (8)$$

To form our solution to Eq. (6), we first approximate the right-hand side of Eq. (8) by the first term, neglecting higher order terms involving $c^{(3)}(\mathbf{r}_1,\mathbf{r}_2,\mathbf{r}_3)$, etc. Therefore, in this work we have approximated the two particle direct correlation function for the modulated liquid by the corresponding quantity for the unmodulated liquid at the same temperature and bulk density for the calculation of the nontrivial singlet particle density. Such an approximation is similar to that used in modern density functional theories of freezing.[19–21] In such theories of freezing the two particle direct correlation function for the solid is approximated by the corresponding quantity for the coexisting liquid. The difference in using this truncated expansion here vs that in the theories of freezing is that here, the bulk density and *thermodynamic phase* of the reference system and the modulated system are necessarily the same. Thus substituting

$$c^{(2)}(\mathbf{r}_1,\mathbf{r}_2) \simeq c_0^{(2)}(r_{12})$$

into Eq. (6) we obtain

$$\nabla_1\{\ln[\rho(\mathbf{r}_1)] + \beta U^{(1)}(\mathbf{r}_1)\} = -\int \rho(\mathbf{r}_2)\nabla_2 c^{(2)}(r_{12})d\mathbf{r}_2 . \quad (9)$$

We now invoke the identity

$$\nabla_2 c_0^{(2)}(r_{12}) = -\nabla_1 c_0^{(2)}(r_{12})$$

and substitute into Eq. (9) to find upon interchanging integration and differentiation:

$$\nabla_1\{\ln[\rho(\mathbf{r}_1)] + \beta U^{(1)}(\mathbf{r}_1)\} = \nabla_1 \int \rho(\mathbf{r}_2)c_0^{(2)}(r_{12})d\mathbf{r}_2 . \quad (10)$$

Equation (10) can be integrated immediately to yield

$$\rho(r_1) = A\exp\{-\beta U^{(1)}(\mathbf{r}_1) + \int c_0^{(2)}(r_{12})\rho(\mathbf{r}_2)d\mathbf{r}_2\}, \quad (11)$$

where A is an integration constant to be determined by Eq. (7). The similarity between Eq. (11) and the corresponding expression for the density functional freezing theories is now evident. Within the approximations outlined above, we can proceed to calculate the experimentally observed structure factors[8–11] for alkali intercalates in graphite by finding the pair correlations in this anisotropic system.

We notice that the experimental structure factors are necessarily measured as a function of only one vector argument in momentum space. The corresponding quantity in real space will not be $g^{(2)}(\mathbf{r}_1,\mathbf{r}_2)$ but an effective radial distribution function given by

$$G(\mathbf{r}) = \frac{1}{\rho_0 N}\int \rho(\mathbf{r}_1)g^{(2)}(\mathbf{r}_1,\mathbf{r}_1+\mathbf{r})\rho(\mathbf{r}_1+\mathbf{r})d\mathbf{r}_1 . \quad (12)$$

The experimental structure factor is then related to the Fourier transform of Eq. (12):

$$S(k) = 1 + \rho_0 \int e^{-i\mathbf{k}\cdot\mathbf{r}}[G(\mathbf{r}) - 1]d\mathbf{r} . \quad (13)$$

For our calculation we perform an expansion of $g^{(2)}$ about an isotropic reference system similar to that in Eq. (8) and again keep only the first term

$$g^{(2)}(\mathbf{r}_1,\mathbf{r}_1+\mathbf{r}) = g_0^{(2)}(r_{12}) + \int \frac{\delta g^{(2)}(\mathbf{r}_1,\mathbf{r}_1+\mathbf{r})}{\delta\rho(\mathbf{r}_2)} \times [\rho(\mathbf{r}_2) - \rho_0]d\mathbf{r}_2 + \cdots .$$

This then is used in the right-hand side of Eq. (12) with the nontrivial singlet density for our system obtained from a solution to Eq. (11).

In the Appendix the strategies for the numerical solution of these equations are described.

III. RESULTS

In order to compare with the experimental data we have chosen a two-dimensional density for the ions of $\rho = 0.029\,26$ ions/Å^2 at a temperature of 300 K. For Rb ions the screening implied for this state yields $\varkappa = 0.49$ Å^{-1} for the potential in Eq. (3). A reasonable estimate of the one body strength parameter, $K = -0.45$ in reduced units, extrapolated from experiment[9] was employed.

Figure 1 presents the results of our calculation for the parameters and thermodynamic state given above in **k** space. The sixfold symmetry of the underlying lattice or one body potential in r space is manifest in the symmetry of $S(k_x,k_y)$. This is a result of the fact that the Fourier transform of a spherical harmonic of given order and rank has the same order and rank. About each reciprocal lattice peak, including the peak at $k_x = k_y = 0$, a distorted set of rings appear. In a simple isotropic fluid there would be only the central Debye–Scherer rings. With the presence of an anisotropic external field, which causes density waves in our system, a replica of the isotropic $S(k)$ is found about each of the reciprocal lattice vector peaks. These rings interfere both constructively and destructively with each other to produce the

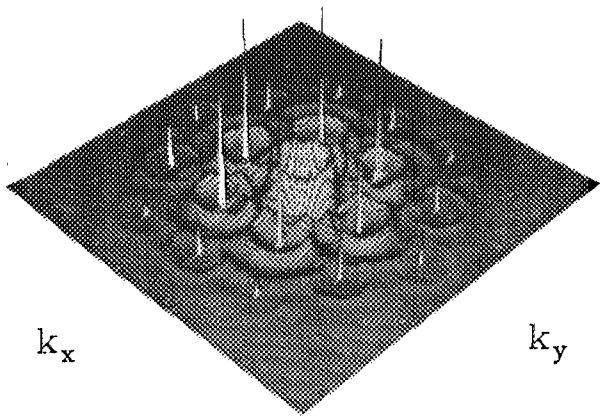

FIG. 1. Structure factor diffraction intensity pattern in two dimensions, $S(k_x,k_y)$. Density $= 0.029\,26$ Å^{-2} and temperature $= 300$ K, see the text for other parameters.

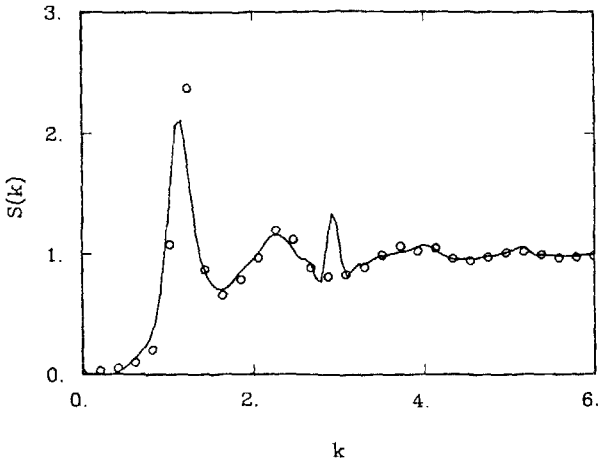

FIG. 2. Isotropic average for structure factor in Fig. 1. Bragg-like features were removed before the averaging.

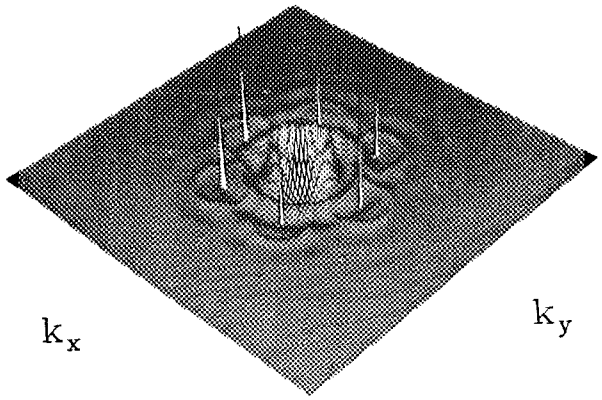

FIG. 4. Same as Fig. 1 with the anisotropy parameter K reduced by a factor of 2. A considerable decrease in the k-space density wave structure is noticed when compared with either Fig. 1 or 3.

noticable variations in intensity of a given ring. The variations also have a sixfold symmetry but the intensity of the variations predicted for a given ring is not uniform. It is not possible to further quantify this point much further from the existing experimental data.

In Fig. 2 we compare our results in **k** space, after performing an isotropic average, with the experimental data for which the sharp "Bragg-like" features were artificially removed. We have done no systematic potential parameter search but clearly the agreement between our trial potential and the experiment is satisfactory. The peak placement and the modulations, which are not found in the isotropic case, are clearly in good agreement. Some discrepancy in the height of the first peak does exist between our results and the experimental data. Our calculations (not shown) and preliminary computer simulation results[22] indicate that a change in the functional form of the pair potential, Eq. (3), will change the intensity of the peaks in $S(k_x,k_y)$. Preliminary indications from computer experiments[22] indicates good agreement with our theory for the peak heights in both **k** space and **r** space for a given potential form and parametrization.

As the temperature is raised, the first ring of structure factor for an isotropic fluid decreases in intensity with little alteration of the placement. A similar behavior is seen in the anisotropic case shown in Fig. 3 where the temperature was raised from 300 to 400 K. A more dramatic change in the intensity of the noncentral rings may be achieved by substantially reducing the strength of the anisotropy. By using a value of K half that used for comparison with experiment we see in Fig. 4 that a substantial reduction in the height of the rings surrounding the high order reciprocal lattice vectors occurs. However, the main Debye–Scherer rings about the origin are quite intact. The higher K is, the larger the intensity of the high order rings. This interplay between U_2 and U_1 is apparent because if we reduce K, we reduce the amplitude of the modulations in $\rho(\mathbf{r})$ and thus the contribution to $G(\mathbf{r})$ in Eq. (12) from $\rho(r)$ is reduced. Clearly for $K=0$ the $S(k_x,k_y)$ given in Eq. (13) will then be the one for a system without an external field. Also, a competition between the length scales is implied by Eqs. (2) and (3) when used in our method. As the intensity of *both* of these terms of the total interaction potential [Eq. (1)] scale with temperature the change in the diffraction pattern with respect to K alone is qualitatively different from that with respect to temperature.

The radius of the k-space rings of all orders is dependent on the total bulk density of ions. Much as in the case of isotropic fluids away from a phase transition, the higher the density, the larger the radius and intensity of the rings. The

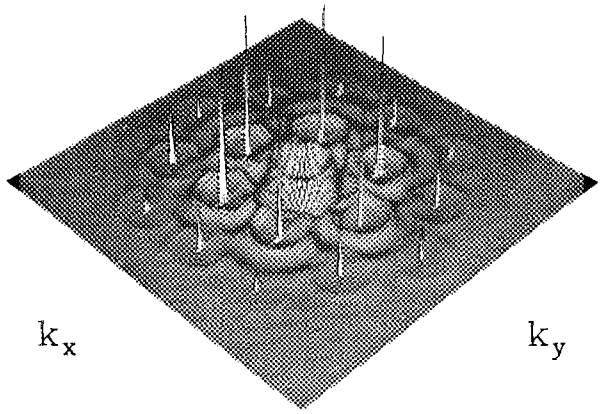

FIG. 3. Same as Fig. 1 with $T=400$ K. Notice the decrease in intensity of the rings from that found at the lower temperature displayed in Fig. 1.

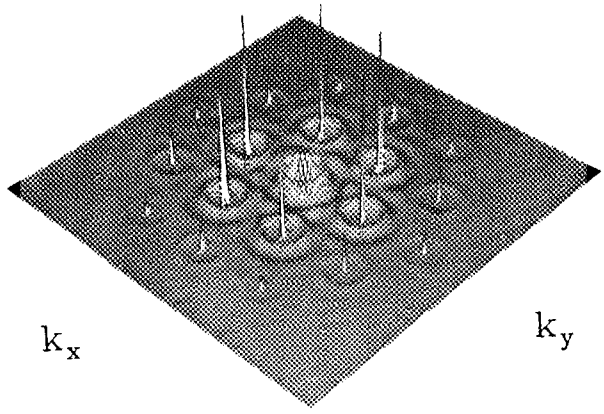

FIG. 5. Same as Fig. 1 with the density ρ reduced by a factor of 2. The density waves are hardly affected by a reduction in packing.

average bulk density directly effects the reference system direct correlation function in r space, $c_0(\mathbf{r}_{12})$. As we change density from ρ_0 to $\rho_0/2$, $c_0(0)$ changes from -35.5 to -27.0. In Fig. 5 the effect on the anisotropic system is demonstrated in k space for a density corresponding to half that of the experimental state. We find the substantial reduction in density effects the heights of all of the rings but that it has a only small effect on the height of the intense Bragg-like peaks. Thus, the density wave structure in the liquid system remains largely intact even for a 50% reduction in density.

This density variation pattern may be understood by considering a partitioning of the terms in Eq. (12). Partitioning $\rho(\mathbf{r}) = n(\mathbf{r}) + \rho_0$ we find

$$G(\mathbf{r}) = \frac{1}{\rho_0^2 V}\int\left\{n(\mathbf{r}_1)n(\mathbf{r}_1+\mathbf{r}) + \rho_0^2\right\}g^{(2)}(\mathbf{r}_1,\mathbf{r}_1+\mathbf{r})d\mathbf{r}_1$$
$$= \frac{1}{V}\int\left\{\frac{n(\mathbf{r}_1)n(\mathbf{r}_1+\mathbf{r})}{\rho_0^2} + 1\right\}g^{(2)}(\mathbf{r}_1,\mathbf{r}_1+\mathbf{r})d\mathbf{r}_1 . \tag{14}$$

If we decrease density, we increase the first term in the brackets above relative to the second term which dictates the contribution of the anisotropic field to $S(k_x,k_y)$. Thus, we may approximately decompose the system into the isotropic contributions given by the second term in brackets in Eq. (40) and the anisotropic interference contributions from the first term.

IV. DISCUSSION AND CONCLUSION

The present study of the interionic structure of synthetic metals of the graphite–alkali intercalation class makes use of a reduction in dimensionality (from 3D to 2D) due to the restraining presence of the essentially impenetrable layers of graphite. Such a method has been used in many other cases in the literature[23] where there existed a strong anisotroy in one (or more) direction. Perhaps the most familiar example is that of monolayer physical adsorption where Steele and co-workers[18,23,24] have used techniques similar in spirit to those applied here to study the structure and thermodynamics of such systems, particularly the freezing transition of adsorbed monolayers.[18] Our efforts have centered on the application of low order density functional theory to interpret the system dependence of the two-dimensional diffraction patterns.

The present low order theory for the symmetry and intensity patterns of the diffraction data for alkali fluids intercalated betweeen the layers of graphite gives excellent qualitative agreement and resonable quantitative agreement with experiment. Preliminary simulation results indicate that better quantitative agreement with experiment can be obtained with a more careful study of model interaction potentials.[22] The use of our theoretical method would clearly be a less time and resource consuming method for modeling parametrization than computer experiments.

ACKNOWLEDGMENTS

The authors thank the Robert A. Welch foundation for support of this work. Professor S. C. Moss and Mr. J. D. Fan are acknowledged for many stimulating conversations.

APPENDIX

Although iterative mixing methods for integral equations have been used for quite awhile in the literature,[6] we have found it useful to view such a technique as a recursive mapping. For this section the use of a subscript shall denote the iteration number. Consider an operator or a mapping f such that $c_n = f(c_{n-1})$. In a case of interest for this work we might view f as an operator in which

$$c_{n-1} \rightarrow \mathrm{OZ} \rightarrow \mathrm{HNC} \rightarrow = c_n . \tag{A1}$$

Clearly, f in this case could have been defined to operate on h_n as well. Formally, the iteration of a set of nonlinear equations in this context defines a recursive relation. We wish to try to find a solution to

$$x_n = f(x_{n-1}) \tag{A2}$$

denoted by x_∞ such that

$$x_\infty = f(x_\infty). \tag{A3}$$

Symbolically, a solution is found if

$$x_n = f(x_{n-1}) = x_{n-1} \Rightarrow x_\infty = f(x_\infty). \tag{A4}$$

We have by addition

$$x_n - x_{n-1} = f(x_{n-1}) - f(x_{n-2}) \tag{A5}$$

by our recursive relation [Eq. (A2)] we may define an approximate finite difference derivitive

$$f(x_{n-1}) - f(x_{n-2}) = f'(x)_{x=\xi_n}(x_{n-1} - x_{n-2}), \tag{A6}$$

where $x_{n-1} < \xi_n < x_{n-2}$. By repeated substitution we obtain

$$x_n - x_{n-1} = f'(\xi_n)f'(\xi_{n-1})f'(\xi_{n-2})\cdots f(\xi_2)(x_2 - x_1). \tag{A7}$$

If $|f'(\xi)_{\max}| < 1.0$ then $\lim_{n\to\infty} x_n = x_\infty$.

However, simple round-off errors can ruin such a scheme so that x_n "passes" x_∞ and eventually diverges numerically. To prevent this for iterative methods, we can include an extrapolation technique.

Consider the difference function

$$y(x) = f(x) - x. \tag{A8}$$

For a solution to our problem $y = f(x_\infty) - x_\infty = 0.0$. For two succesive iterations by our recursive relation we obtain

$$y(x_1) = f(x_1) - x_1 = x_2 - x_1 \tag{A9}$$

and

$$y(x_2) = f(x_2) - x_2 = x_3 - x_2. \tag{A10}$$

Thus, if $y(x_1)$ has different sign from $y(x_2)$, there should be a solution x_∞ in between x_1 and x_2. We may approximate $\delta y/\delta x \simeq constant$ for a sufficiently small range of x. Therefore

$$\frac{y(x_2) - y(x_1)}{x_2 - x_1} = \frac{y(x_\infty) - y(x_1)}{x_\infty - x_1}. \tag{A11}$$

Since $y(x_\infty) = 0$, the linear extrapolation to the solution is given by

$$x_\infty = x_1 - \frac{y(x_1)(x_2 - x_1)}{y(x_2) - y(x_1)}$$

$$= x_1 - \frac{(x_2 - x_1)(x_2 - x_1)}{x_3 - x_2 - (x_2 - x_1)}. \quad \text{(A12)}$$

A similar form has been given by Broyles[25] for the restrictive assumption of monotonically and exponentially decreasing residuals. After every two iterations our extrapolation may be applied to speed the convergence with very little computational effort. The advantage of this method is that it will automatically search for the correct direction in our recursive solution space to reach the destination. The outcome of our testing has shown that it worked very efficiently for equations that are not very stiff. However, for stiff equations the solution will diverge rapidly even with our extrapolation technique.

Classically, to prevent x from diverging one employs the so-called "mixture method" first introduced to liquid state integral equations by Broyles[25] in conjunction with the solution to the Born–Green[16] equation.

For mixing, in addition to the recursive relation [Eq. (A2)], we have

$$x_{n+1} = \alpha x_n + \beta f(x_n), \quad \text{(A13)}$$

where traditionally $\alpha + \beta = 1$ and $\alpha, \beta > 0$.

We can use the extrapolation procedure in conjunction with this method. Proceeding as before for two succesive iterations we have

$$x_n = \alpha x_{n-1} + \beta f(x_{n-1}) \quad \text{(A14)}$$

and

$$x_{n-1} = \alpha x_{n-2} + \beta f(x_{n-2}). \quad \text{(A15)}$$

Subtracting these expressions one obtains

$$x_n - x_{n-1} = \alpha(x_{n-1} - x_{n-2}) + \beta [f(x_{n-1}) - f(x_{n-2})] \quad \text{(A16)}$$

used in conjunction with the finite difference derivative expression

$$f(x_{n-1}) - f(x_{n-2}) = f'(\xi_{n-1})(x_{n-1} - x_{n-2}) \quad \text{(A17)}$$

yields a similar expression to that derived earlier that takes account of mixing

$$x_n - x_{n-1} = [\beta f'(\xi_{n-1}) + \alpha][\beta f'(\xi_{n-2}) + \alpha] \cdots [\beta f'(\xi_2) + \alpha][x_2 - x_1]. \quad \text{(A18)}$$

In analogy to Eq. (26) we obtain

$$x_\infty = x_i - \frac{(x_{i+1} - \alpha x_{i-1} - \beta x_i)(x_{i+1} - x_i)}{x_{i+2} - x_{i+1}(\beta + 1) + x_i(\beta - \alpha) + \alpha x_{i-1}}. \quad \text{(A19)}$$

In this case the requirement we need to have is

$$|\beta f'(x) + \alpha| < 1 \quad \text{(A20)}$$

for a solution.

Consider the case for $\beta > 0$

$$1 - \frac{2}{\beta} < f'(x) < 1. \quad \text{(A21)}$$

For a function like the HNC closure $f'(x) > 0$ and one can employ a value of β all the way up to 2. This implies an $\alpha = -1$. This "overmixture" is analogous to over relaxation techniques use for differential operators. In several simple cases a negative α alone, without the extrapolation step, can improve the convergence speed by a factor of 4 to 5.

We can define a convergence parameter s as a generalization of Eq. (A20):

$$|\beta f'(x) + \alpha| = s, \quad \text{(A22)}$$

where $s < 1.0$. Then we have

$$\beta = \frac{1 \pm s}{1.0 - f'(x)}.$$

For stiff equations β frequently has to be small to prevent numerical divergences and so s has to be near 1.0. However, a small β slows down convergence. By analogy with Eqs. (A7) and (A18) we have

$$x_n - x_{n-1} = s_n s_{n-1} s_{n-2} \cdots s_1 (x_2 - x_1). \quad \text{(A23)}$$

Thus, the best speed of convergence obtains when β can be chosen as follows:

$$\beta_p = \frac{1}{1 - f'(x)}. \quad \text{(A24)}$$

For the HNC closure, since $f'(x) > 0$, β_p is bigger than 1, thus it may converge faster with β greater than 1. We may reduce our method to a familiar form by substitution of the expression for β_p:

$$x_n = (1 - \beta_p)x_{n-1} + \beta_p f(x_{n-1}) = \left(1 - \frac{1}{1 - f'(x)}\right)x_{n-1} + \frac{1}{1 - f'(x)} f(x_{n-1}). \quad \text{(A25)}$$

Thus, in this case, the method is essentially reduced to a functional variant of Newton's method for the difference function y in Eq. (A7).

Clearly there are some natural bounds on β:

$$\beta_{\min} = 0, \quad \text{(A26)}$$

$$\beta_{\max} = \frac{2}{1 - f'(x)}. \quad \text{(A27)}$$

As long as $[1 - f'(x)]$ has a definite sign and a maximum, we can always pick a small β in between $\beta_{\min}$ and $\beta_{\max}$ to make our scheme convergent. It is clear that the optimal *beta* is a function of the iteration number for a given problem and starting guess because of the dependence on $f'(x)$. So, following Eq. (A24), a linear approximation that is quite useful is

$$\beta_n = (1 \pm s)[1 - f'_n(x)]^{-1}.$$

The above discussion is not restricted to the current problem of a nonlinear integral equation for two-dimensional anisotropic fluids but also can be extended to many other calculations. Currently, these methods are also being applied to a variety of three-dimensional isotropic fluid problems for both ionic and molecular systems.[26]

[1] H. Kamimura, Physics Today **40**, (No. 12), 64 (1987).
[2] M. Plischke, Can. J. Phys. **59**, 802 (1981).
[3] D. P. DiVincenzo, Synt. Met. **12**, 111 (1985).

[4]O. A. Karim and B. M. Pettitt, Chem. Phys. Lett. **137**, 72 (1987).
[5]K. Tamaru, Catal. Rev. **4**, 161 (1970).
[6]I. M. Panayotou and I. B. Rashkou, J. Poly. Sci. Part A **10**, 1267 (1972).
[7]T. Ohno and H. Kamimura, J. Phys. Soc. Jpn. **52**, 223 (1983).
[8]F. Rousseaux, R. Moret, D. Guerard, P. Lagrange, and M. Lelaurin, Synth. Met. **12**, 45 (1985).
[9]S. C. Moss, G. Reiter, J. L. Robertson, C. Thompson, J. D. Fan, and K. Ohskima, Phys. Rev. Lett. **57**, 3191 (1986).
[10]R. Clarke, N. Caswell, S. A. Solin, and P. M. Horn, Phys. Rev. Lett. **43**, 2018 (1979).
[11]H. Zabel, S. C. Moss, N. Caswell, and S. A. Solin, Phys. Rev. Lett. **43**, 2022 (1979).
[12]D. P. DiVincenzo and S. Rabii, Phys. Rev. B **25**, 411 (1982).
[13]N. A. W. Holzwarth, S. G. Louie, and S. Rabii, Phys. Rev. B **28**, 1013 (1983).
[14]M. E. Preil and J. E. Fischer, Phys. Rev. Lett. **52**, 1141 (1984).
[15]D. P. DiVincenzo and E. J. Mele, Phys. Rev. B **32**, 2538 (1985).
[16]J. P. Hansen and I. R. McDonald, *Theory of Simple Liquids* (Academic, New York, 1976).
[17]R. Lovett, C. Y. Mou, and F. P. Buff, J. Chem. Phys. **65**, 570 (1976).
[18]S. Sokolowski and W. Steele, J. Chem. Phys. **82**, 2499 (1985).
[19]T. V. Ramakrishnan and M. Yussouff, Phys. Rev. B **14**, 2775 (1979).
[20]D. W. Oxtoby and A. D. J. Haymet, J. Chem. Phys. **74**, 2559 (1981).
[21]K. Ding, D. Chandler, S. J. Smithline, and A. D. J. Haymet, Phys. Rev. Lett. **59**, 1698 (1987); S. J. Smithline, S. W. Rick, and A. D. J. Haymet, J. Chem. Phys. **88**, 2004 (1988).
[22]J. D. Fan, O. A. Karim, G. Reiter, and S. C. Moss, Phys. Rev. Lett. (submitted).
[23]W. A. Steele, *The Interaction of Gases with Solid Surfaces* (Pergamon, New York, 1974), Chap. 4.
[24]P. A. Monson, W. Steele, and D. Henderson, J. Chem. Phys. **74**, 6431 (1981).
[25]A. A. Broyles, J. Chem. Phys. **33**, 456 (1960).
[26]Z. M. Chen and B. M. Pettitt (work in progress).